Photoinduced $\chi^{(2)}$ for second harmonic generation in stoichiometric silicon nitride waveguides

Marco A. G. Porcel[1], Jesse Mak[1], Caterina Taballione[1], Victoria K. Schermerhorn[1], Jörn P. Epping[2], Peter J.M. van der Slot[1], and Klaus-J. Boller[1]

[1]Laser Physics and Nonlinear Optics Group, MESA$^+$ Institute for Nanotechnology, University of Twente, Enschede 7500 AE, The Netherlands
[2]LioniX International B.V., PO Box 456, Enschede 7500 AL, The Netherlands

ABSTRACT

We present for the first time second harmonic generation in amorphous stoichiometric Si_3N_4 waveguides grown via low pressure chemical vapor deposition. An effective second-order susceptibility ($\chi^{(2)}$) is established via the coherent photogalvanic effect. A waveguide was designed to phase match a horizontally (parallel to the waveguide width) polarized hybrid EH_{00} mode at 1064 nm with the higher-order hybrid transverse EH_{02} mode at 532 nm. A mode-locked laser delivering 6.2-ps pulses at 1064 nm with a repetition rate of 20 MHz was used as pump. When pumped with a constant average power, it was found that the photoinduced $\chi^{(2)}$ is established over a time of the order of 1000 s in as-manufactured waveguides, during which the second harmonic signal grows from below noise to a saturation value. The life-time of the photoinduced $\chi^{(2)}$ is at least a week. In steady state, we obtain a maximum conversion efficiency close to 0.4% for an average pump power of 13 mW inside the waveguide. The effective second-order susceptibility is found to be 8.6 pm/V.

Keywords: Integrated nonlinear optics, second harmonic generation, photoinduced second-order susceptibility, stoichiometric silicon nitride

1. INTRODUCTION

Stoichiometric silicon nitride (Si_3N_4) waveguides, grown via low pressure chemical vapour deposition (LPCVD), are a stable and versatile photonics platform characterized by a low propagation loss, a broad transparency range, from the visible to the mid-infrared,[1–3] and reproducible material dispersion.[4,5] The recent demonstrations of the broadest-ever optical spectrum on a chip with this specific platform, 495 Thz[6] when pumped at 1064 nm and 453 THz[7] when pumped at 1550 nm, has opened a wide prospective towards third-order nonlinear functionalities, e.g., four-wave mixing,[8] frequency comb generation[9] and the possibility of efficient all-optical switching.[10] However, a great number of additional functionalities would become possible in such a platform if a second-order susceptibility, $\chi^{(2)}$, would be available.

In principle, SiN, grown either via RF-sputtering or chemical vapour deposition, is amorphous and therefore has no bulk second-order nonlinear response. Nonetheless, second order processes have been observed in thin films[11,12] and waveguide ring resonators.[13] A maximum conversion efficiency of 0.14% was achieved using SiN ring resonators[13] and Bragg gratings [12] to enhance the fundamental and second harmonic fields. Proposed origins for the presence of a bulk effective second order nonlinearity are silicon clusters[11] and dangling bonds.[14]

Here, we present the first observation of second harmonic generation (SHG) resulting from a photoinduced $\chi^{(2)}$ in LPCVD stoichiometric Si_3N_4 waveguides. When pumped with a constant average power at 1064 nm, it was found that the photoinduced $\chi^{(2)}$ is established over a time of the order of 1000 s in as-manufactured stoichiometric Si_3N_4 waveguides, during which the second harmonic signal at 532 nm grows from below noise to a saturation value. The observed build-up of an effective second order susceptibility is best explained by a coherent photogalvanic effect, similar to what has been observed in phosphor doped fibers[15,16] and glasses.[17–19] The life-time of the photoinduced $\chi^{(2)}$ is found to be at least a week.

Further author information: E-mail: p.j.m.vanderslot@utwente.nl

Nonlinear Optics and Applications X, edited by Mario Bertolotti, Joseph W. Haus, Alexei M. Zheltikov, Proc. of SPIE Vol. 10228, 102280R · © 2017 SPIE · CCC code: 0277-786X/17/$18 · doi: 10.1117/12.2265797

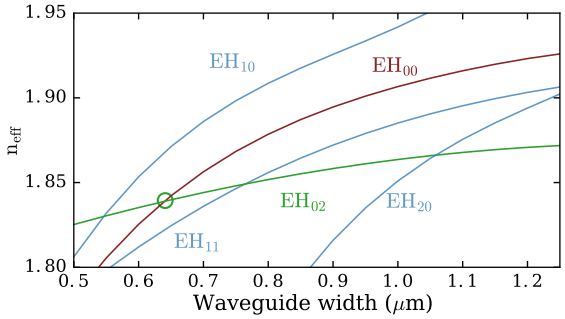

Figure 1. Calculated effective refractive index for the fundamental mode at 1064 nm (red line), the hybrid EH_{20} mode at 532 nm (green line), and selected higher-order hybrid modes at 532 nm (blue lines). All transverse modes are horizontally polarized (parallel to the waveguide width). The circle marks the waveguide width that allows phase-matching by modal dispersion.

2. REQUIREMENTS FOR SECOND HARMONIC GENERATION

Two fundamental conditions need to be fulfilled for second harmonic generation. Firstly, the material needs to possess a second-order nonlinear susceptibility ($\chi^{(2)}$). Secondly, phase-matching between the fundamental radiation and its second harmonic is needed. The latter can be realized by engineering the waveguide cross-section for phase-matching by modal dispersion,[20] such that the effective refractive index of the fundamental mode at a frequency matches the effective refractive index of a higher order transverse mode at the doubled frequency. In order to support higher-order transverse modes we consider waveguides with a large area core. In the remainder of this manuscript we will limit ourselves to waveguides with a fixed height of 1 μm and with widths varying from 0.6 to 1.2 μm in steps of 0.1 μm. Furthermore, the polarization of the pump light is fixed and chosen to be horizontal (parallel to the width of the waveguide). Figure 1 shows the effective refractive index for the fundamental mode at the pump wavelength of 1064 nm (red line) and the effective refractive index of the next higher transverse mode at the second harmonic wavelength of 532 nm (green line) as a function of the waveguide width. For the calculations, we considered a step index refractive index profile that includes the measured shape of the waveguide core,[4] and the material dispersion for stoichiometric Si_3N_4 and silica was taken from Luke et al.[3] The effective refractive index of a few selected higher-order transverse modes at the second harmonic wavelength (blue lines) are also plotted. Note, the polarization of the second harmonic wave is taken to be the same as that of the fundamental wave, i.e., horizontal. The open circle in Fig. 1 indicates the width of the core for which the effective refractive index for the fundamental EH_{00} hybrid mode (at 1064 nm) equals that of the higher transverse EH_{02} hybrid mode (at 532 nm), and modal phase matching is expected for this waveguide width.

The other requirement for second harmonic generation is the presence of a $\chi^{(2)}$, which is absent in bulk centrosymmetric materials like stoichiometric Si_3N_4 waveguides. Only very close to the interface between the core and cladding, where the symmetry is broken, the $\chi^{(2)}$ is non-zero. However, for the high-confinement Si_3N_4 waveguides needed for modal phase matching, the magnitude of the optical field near the interface is small and no SHG is expected. The symmetry of the waveguide material may also be broken in other ways, e.g., by applying stress to the waveguide. Here, we show that the coherent photogalvanic effect can be used to induce a long-lived internal charge separation that breaks the material symmetry and can generate an effective $\chi^{(2)}_{\text{eff}}$.[15,17–19,21,22]

3. EXPERIMENTAL SETUP

To obtain modal phase matching, the waveguide needs to support higher-order transverse modes, which requires a large area core. Such high confinement LPCVD Si_3N_4 waveguides can be manufactured using a process described by Epping et al.[4] Using this process a set of waveguides was manufactured with a height of the Si_3N_4 core of 1 μm, varying widths, w, ranging from 0.6 to 1.2 μm in steps of 0.1 μm, and various lengths, L.

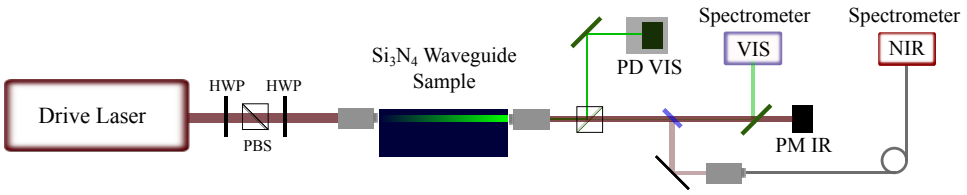

Figure 2. Schematic view of the experimental setup. The drive laser consists of a mode-locked 1064-nm laser delivering 6.2-ps pulses with a repetition rate of 20 MHz coupled through two half-wave plates (HWP) and a polarizing beam splitter (PBS) and focused into a waveguide using an aspheric lens (AL). After the waveguide, the light is collected using a microscope objective, spectrally separated and subsequently guided to a photodiode (PD) and a power meter to measure the average SH and infrared power, respectively. A small portion of the power (1% of SH and 16% of IR) is guided into two spectrometers to monitor the visible (VIS) and infrared (NIR) spectra.

The experimental setup used to observe second harmonic generation in these waveguides is schematically shown in Fig. 2. As pump we use a mode-locked Yb-doped fiber laser operating at a wavelength of 1064 nm with a pulse duration of 6.2 ps and a repetition rate of 20 MHz. The power of the laser is controlled via a half-wave plate (HWP) and a polarizing beam splitter (PBS). The second HWP is used to align the polarization to the width of the waveguide (horizontal polarization). Due to the high numerical aperture (NA) of the waveguide, an aspheric lens with a NA of 0.68 was used to couple the pump light into the waveguide. The coupling loss is measured to be 7 dB. After the waveguide, a microscope objective with a NA of 0.75 is used to collect the light, which is subsequently spectrally separated and guided to a photodiode (PD) and power meter (PM) to measure the SH and fundamental power, respectively. A small fraction of the power, 1% and 16% for the SH and fundamental, respectively, is guided into two spectrometers to simultaneously monitor the IR and SH spectrum.

4. PHOTOINDUCED GENERATION OF $\chi^{(2)}$

As discussed, modal phase matching is expected to happen for a specific waveguide width of $w = 0.65$ μm. However, as shown in Fig. 3, we observed SHG for various waveguide widths. In Figs. 3a-d we plot the pump power, P_{IR}, (red line) coupled into the waveguide and the output power at the second harmonic frequency, P_{SH}, (green line) as a function of time for four as-manufactured waveguides with widths and lengths as indicated in the figure. This figure shows that for a constant pump power the second harmonic power grows from below noise to a saturated value over a time that varies from 600 to 2×10^4 seconds when the average pump power in the waveguide ranges from 6 to 1 mW. We have observed this effect in all as-manufactured waveguides investigated. Once a waveguide has been exposed to a sufficiently strong IR pump light, turning the pump off and then on again results in immediate generation of the saturated SH wave.

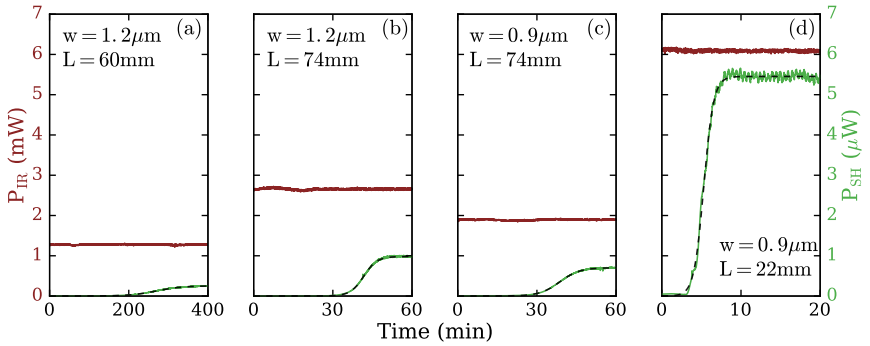

Figure 3. Average pump power P_{IR} at 1064 nm (red line) at the entrance of the waveguide and second harmonic power P_{SH} at 532 nm (green line) at the output measured as a function of time for a waveguide of width, w, and length, L, as indicated in figures 3a-d. The dashed black line is the fit for the average second harmonic power using the phenomenological model.

A similar observation of second harmonic generation was first reported by Österberg et al.[21] in phosphor-doped silica fibers. The creation of a second-order nonlinear susceptibility in the amorphous material was thought to be due to a coherent photogalvanic effect,[23] and this idea was further supported by later research.[15,17–19,22] The coherent photogalvanic model assumes that initially a small SH wave is generated. This SH wave will produce a DC electric field $\mathcal{E}_{DC}$ via the third-order susceptibility, $\chi^{(3)}$ according to[22,24]

$$\mathcal{E}_{DC} \propto \chi^{(3)}|E(\omega)|^2 E(2\omega)cos(\Delta kz), \tag{1}$$

where $E(\omega)$ and $E(2\omega)$ are the field strengths at the fundamental and second harmonic frequency, respectively, z is the propagation distance and $\Delta k = 2k_\omega - k_{2\omega}$ is the phase mismatch. This DC field, together with a nonlinear optical resonant enhancement of the electrical conductivity, will induce a charge separation, which breaks the symmetry of the centrosymmetric amorphous material. The internal field E_{DC} associated with the charge separation will together with the third order susceptibility create an effective second-order susceptibility given by[22,24]

$$\chi^{(2)}_{\text{eff}} = \chi^{(3)} E_{DC}. \tag{2}$$

Note, in absence of the optical fields, there is no nonlinear optical enhancement of the electrical conductivity and the charge mobility is greatly reduced, leading to a long-lived induced charge separation. Equation 1 shows that the induced nonlinear field $\mathcal{E}_{DC}$ has a spatial periodicity given by the phase mismatch between the fundamental and the second harmonic. Consequently, the effective second order susceptibility $\chi^{(2)}_{\text{eff}}$ will possess the same spatial periodicity, which means that second harmonic generation enabled by $\chi^{(2)}_{\text{eff}}$ is automatically quasi-phase matched. This explains why we observed second harmonic generation for all widths of the waveguides investigated. The life-time of the photoinduced second-order susceptibility is observed to be longer than one week, in agreement with observations made by others in fibers and glass.[15–17,21]

Various phenomenological models have been used to describe the coherent photogalvanic effect.[17,22,25] We use the time-dependent phenomenological model by Balakirev et al.[25] to describe the growth of $\chi^{(2)}_{\text{eff}}$ with time. The fit of this model to the experimental data is shown as a dashed line in Figs. 3a-d. The agreement between the model and the experimental data is excellent, which further supports the coherent photogalvanic effect as source of the effective second-order susceptibility.

5. STEADY-STATE SECOND HARMONIC GENERATION

Now that the generation of an effective second order susceptibility based on the coherent photogalvanic effect has been discussed, we investigate the properties of the second harmonic signal in the stationary state (i.e., after the $\chi^{(2)}_{\text{eff}}$ is fully developed). One property of the SH signal is that its power should be proportional to the fundamental power squared, $P_{2\omega}(t) = cP_\omega(t)^2$. The measured SH power is plotted in Fig. 4 as a function of the

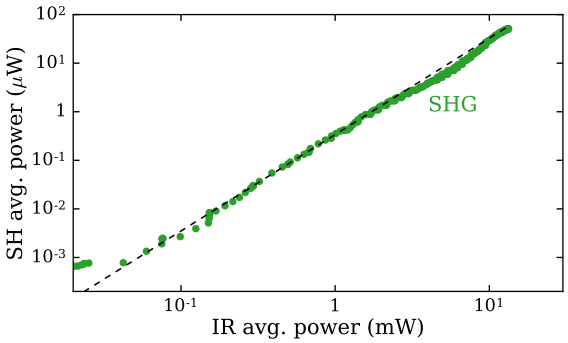

Figure 4. Measured average power at 532 nm as a function of average power inside the waveguide at 1064 nm. The waveguide used has a width of 0.9 μm, a height of 1.0 μm and a length of 22 mm. The line is a least-square fit to the data and has a slope of 1.98±0.016.

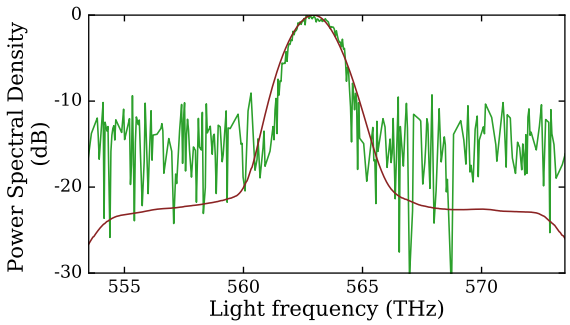

Figure 5. Measured spectral power density of the SH signal (green line) and scaled autocorrelation signal of the IR pump spectrum (red line), both normalized with respect to its maximum. Both spectra were measured at the output of the waveguide.

fundamental power at the entrance of the waveguide with $w = 0.9$ μm and $L = 22$ mm. The dashed line is a least square fit to the data and has a slope of 1.98 ± 0.02, showing the expected quadratic growth of the SH power with IR power. The proportionality constant c has been determined from the fitted line. The solution of the nonlinear coupled-mode equations for waveguides,[20] under the assumption of exact quasi-phase matching, is used to calculate $\chi^{(2)}_{\text{eff}}$ from c, resulting in a value of $\chi^{(2)}_{\text{eff}} = 8.6 \pm 0.6$ pm/V. This value for $\chi^{(2)}_{\text{eff}}$ is similar to that observed in silicon-rich silicon nitride,[11] but larger than the values found when using resonators based on silicon nitride micro rings[13] or Bragg gratings in silicon nitride thin films.[12] The highest average SH power measured is 51 μW for an average pump power of 13 mW, corresponding to a conversion efficiency of 0.4%. To our knowledge, this is the highest conversion efficiency observed in stoichiometric silicon nitride waveguides.

Given that $P_{2\omega}(t)$ is proportional to $P_{\omega}(t)^2$, we expect the spectrum of the SH signal to be similar to the autocorrelation of the IR spectrum scaled to the second harmonic frequency by doubling the IR frequency. Figure 5 shows the measured spectral power density of the second harmonic signal (green line) and the scaled autocorrelation of the IR spectrum of the transmitted pump pulse for a waveguide with $w = 0.6$ μm and $L = 36$ mm when pumped with an averaged power of 2 mW inside the waveguide. Each signal is normalized with respect to its maximum. We observe an excellent agreement between the measured spectrum of the second harmonic signal and the autocorrelation of the pump spectrum, indicating again that second harmonic generation is taking place inside the waveguide. Figure 5 shows a quasi-phase matching bandwidth of 2 THz at -3 dB level.

6. CONCLUSIONS

We have presented for the first time second harmonic generation in stoichiometric LPCVD Si_3N_4 waveguides. The required second order susceptibility is written in these waveguide via the coherent photogalvanic effect, without any external second harmonic seeding. An effective second-order susceptibility is established in a time of the order of 1000 s in as-manufactured waveguides, depending on the average pump power used. During this time, the second harmonic signal builds up from noise to a saturated value. This process leads to an automatic quasi-phase matching of the SHG nonlinear process. Consequently, SHG is observed for all widths of the waveguides investigated. The observed SHG process has a maximum conversion efficiency of 0.4% for an average pump power of 13 mW inside the waveguide, which is, to our knowledge, the highest conversion efficiency achieved in integrated silicon nitride waveguides. The effective second-order susceptibility $\chi^{(2)}_{\text{eff}}$ derived from our measurements is 8.6±0.6 pm/V, similar to that achieved in silicon-rich SiN[11] and larger than observed using periodically etched gratings in SiN films[12] and using SiN ring resonators.[13]

ACKNOWLEDGMENTS

We thank Richard Mateman from LioniX International B.V. for manufacturing the waveguides used in this research. This work is supported by NanoNextNL, a micro and nanotechnology consortium of the Government of the Netherlands and 130 partners, and by the Dutch Technology Foundation STW, which is part of the

Netherlands Organisation for Scientific Research (NWO), and which is partly funded by the Ministry of Economic Affairs.

REFERENCES

[1] Bauters, J. F., Heck, M. J. R., John, D., Dai, D., Tien, M.-C., Barton, J. S., Leinse, A., Heideman, R. G., Blumenthal, D. J., and Bowers, J. E., "Ultra-low-loss high-aspect-ratio Si3N4 waveguides," *Opt. Express* **19**(4), 3163–3174 (2011).

[2] Spencer, D. T., Bauters, J. F., Heck, M. J. R., and Bowers, J. E., "Integrated waveguide coupled Si3N4 resonators in the ultrahigh-Q regime," *Optica* **1**, 153–157 (2014).

[3] Luke, K., Okawachi, Y., Lamont, M. R. E., Gaeta, A. L., and Lipson, M., "Broadband mid-infrared frequency comb generation in a Si3N4 microresonator," *Opt. Lett.* **40**, 4823–4826 (2015).

[4] Epping, J. P., Hoekman, M., Mateman, R., Leinse, A., Heideman, R. G., van Rees, A., van der Slot, P. J., Lee, C. J., and Boller, K.-J., "High confinement, high yield Si3N4 waveguides for nonlinear optical applications," *Opt. Express* **23**(2), 642–648 (2015).

[5] Wrhoff, K., Heideman, R. G., Leinse, A., and Hoekman, M., "TriPleX: a versatile dielectric photonic platform," *AOT* **4** (2015).

[6] Epping, J. P., Hellwig, T., Hoekman, M., Mateman, R., Leinse, A., Heideman, R. G., van Rees, A., van der Slot, P. J., Lee, C. J., Fallnich, C., and Boller, K.-J., "On-chip visible-to-infrared supercontinuum generation with more than 495 THz spectral bandwidth," *Opt. Express* **23**(15), 19596–19604 (2015).

[7] Porcel, M. A. G., Schepers, F., Epping, J. P., Hellwig, T., Hoekman, M., Heideman, R. G., van der Slot, P. J. M., Lee, C. J., Schmidt, R., Bratschitsch, R., Fallnich, C., and Boller, K.-J., "Two-octave spanning supercontinuum generation in stoichiometric silicon nitride waveguides pumped at telecom wavelengths," *Opt. Express* **25**, 1542–1554 (2017).

[8] Epping, J. P., Kues, M., van der Slot, P. J., Lee, C. J., Fallnich, C., and Boller, K.-J., "Integrated CARS source based on seeded four-wave mixing in silicon nitride," *Opt. Express* **21**(26), 32123–32129 (2013).

[9] Pfeifle, J., Brasch, V., Lauermann, M., Yu, Y., Wegner, D., Herr, T., Hartinger, K., Schindler, P., Li, J., Hillerkuss, D., Schmogrow, R., Weimann, C., Holzwarth, R., Freude, W., Leuthold, J., Kippenberg, T. J., and Koos, C., "Coherent terabit communications with microresonator Kerr frequency combs," *Nat Photon* **8**, 375–380 (2014).

[10] Hellwig, T., Epping, J. P., Schnack, M., Boller, K.-J., and Fallnich, C., "Ultrafast, low-power, all-optical switching via birefringent phase-matched transverse mode conversion in integrated waveguides," *Opt. Express* **23**, 19189–19201 (2015).

[11] Kitao, A., Imakita, K., Kawamura, I., and Fujii, M., "An investigation into second harmonic generation by Si-rich SiN $_x$ thin films deposited by RF sputtering over a wide range of Si concentrations," *J. Phys. D: Appl. Phys.* **47**, 215101 (2014).

[12] Ning, T., Pietarinen, H., Hyvrinen, O., Kumar, R., Kaplas, T., Kauranen, M., and Genty, G., "Efficient second-harmonic generation in silicon nitride resonant waveguide gratings," *Opt. Lett.* **37**(20), 4269–4271 (2012).

[13] Levy, J. S. and Lipson, M., "Harmonic generation in silicon nitride ring resonators," *Optics express* **17**(14), 11366–11370 (2011).

[14] Ning, T., Pietarinen, H., Hyvrinen, O., Simonen, J., Genty, G., and Kauranen, M., "Strong second-harmonic generation in silicon nitride films," *Appl. Phys. Lett.* **100**(16), 161902 (2012).

[15] Margulis, W. and Österberg, U., "Second-harmonic generation in optical glass fibers," *JOSA B* **5**(2), 312–316 (1988).

[16] Stolen, R. H. and Tom, H. W. K., "Self-organized phase-matched harmonic generation in optical fibers," *Opt. Lett.* **12**(8), 585–587 (1987).

[17] Dianov, E. M. and Starodubov, D. S., "Photoinduced generation of the second harmonic in centrosymmetric media," *Quant. Electron.* **25**(5), 395–407 (1995).

[18] Sulimov, V. B., "Theory of the coherent photovoltaic effect and the method of nonequilibrium Green's functions," *Zh. ksp. Teor. Fiz* **101**, 1749–1771 (1992).

[19] Balakirev, M. K., Kityk, I. V., Smirnov, V. A., Vostrikova, L. I., and Ebothe, J., "Anisotropy of the optical poling of glass," *Phys. Rev. A* **67**(2) (2003).
[20] Suhara, T. and Fujimura, M., [*Waveguide Nonlinear-Optic Devices*], vol. 11 of *Springer Series in Photonics*, Springer Berlin Heidelberg, Berlin, Heidelberg (2003).
[21] Österberg, U. and Margulis, W., "Experimental studies on efficient frequency doubling in glass optical fibers," *Opt. Lett.* **12**(1), 57–59 (1987).
[22] Anderson, D. Z., Mizrahi, V., and Sipe, J. E., "Model for second-harmonic generation in glass optical fibers based on asymmetric photoelectron emission from defect sites," *Opt. Lett.* **16**(11), 796–798 (1991).
[23] Dianov, E. M. and Kazanski, "Problem of the photoinduced second harmonic generation in optical fibers," *Sov. J. Quantum Electron.* **19**, 575–576 (1989).
[24] Chmela, P., "Preparation of optical fibers for effective second-harmonic generation by the poling technique," *Opt. Lett.* **16**(7), 443–445 (1991).
[25] Balakirev, M. K., Vostrikova, L. I., Smirnov, V. A., and Entin, M. V., "Relaxation of the optical density of glass modulated with bichromatic radiation," *JETP* **63**(3), 176–181 (1996).